

# Towards a guided atom interferometer based on a superconducting atom chip

T Müller<sup>1,2</sup>, X Wu<sup>1</sup>, A Mohan<sup>1</sup>, A Eyvazov<sup>1</sup>, Y Wu<sup>1</sup> and R Dumke<sup>1</sup>

<sup>1</sup> Division of Physics and Applied Physics, School of Physical and Mathematical Sciences, Nanyang Technological University, Singapore 637371, Singapore

<sup>2</sup> Physics Department, Faculty of Science, National University of Singapore, Singapore 117542, Singapore

E-mail: mueller@ntu.edu.sg

**Abstract.** We evaluate the realization of a novel geometry of a guided atom interferometer based on a high temperature superconducting microstructure. The interferometer type structure is obtained with a guiding potential realized by two current carrying superconducting wires in combination with a closed superconducting loop sustaining a persistent current. We present the layout and realization of our superconducting atom chip. By employing simulations we discuss the critical parameters of the interferometer guide in particular near the splitting regions of the matter waves. Based on measurements of the relevant chip properties we discuss the application of a compact and reliable on-chip atom interferometer.

## 1. Introduction

Superconductor technology combined with atom optical systems will allow a new generation of fundamental experiments and novel applications possibly reaching to the pairing of quantum solid state devices with neutral atoms on the quantum mechanical level [1, 2]. In particular, the enormous capability of superconducting devices paired with atom optics is especially promising utilizing microstructured surface traps. For example these can be used for quantum state transfer between solid state and atomic systems [1] or quantum information processing [2]. Microstructured surface trapping and manipulation devices, so-called "atom chips" [3, 4], have proven their great capability and flexibility in the field of ultra-cold atom experiments over the last years. These elements which allow the generation of steep trapping potentials use current carrying wires [5] or permanent magnetic structures [6] as well as micro-optical devices [7]. They have for example been used for guiding and transportation potentials of various kinds [10, 11, 12] as well as for the generation of quantum-degenerate gases [8, 9]. Additionally, the manipulation of neutral atoms with microstructured elements is a promising approach for realizing systems suitable for quantum information processing [13]. Recently, superconducting micro-structured elements have been successfully employed in atom-optics experiments [14, 15, 16].

A major application would be a guided chip-based atom interferometer: In comparison to optical interferometers, atom interferometers have the potential of being several orders of magnitude more sensitive for some applications or giving access to classes of interferometric measurements not possible with optical interferometry in principle [17]. Because of the high intrinsic sensitivity, these interferometers have to be built in a robust way to be applicable under a wide range of environmental conditions.

A new approach to meet this challenge lies in the development of miniaturized and integrated atom optical setups based on micro-fabricated guiding structures. First experiments have been carried out investigating chip based interferometer structures [18, 19, 20]. However, with the traditional atom chips based on metallic conductors at room temperature a symmetric closed Mach-Zehnder interferometer type guiding structure has not been realized. These structures based on normal conductors have always connections to external power sources impeding an ideally symmetric potential. However, the symmetry is one major ingredient of guided atom interferometry. Until now, only radio-frequency dressing [19, 21] or optical approaches [22] realizing the beam-splitting as well as hybrid types of guided atom interferometers which use magnetic confinement in combination with optical beam-splitting pulses [18] can overcome this limitation.

In this article we present the experimental design of a ceramic-based high-temperature superconductor (HTS) atom interferometer chip structure using a persistent current loop to overcome limitations which normal conductors are facing. In combination with two superconducting wires carrying an externally supplied current an atom guide is realized. Along the atomic propagation direction this guide is split into

two arms. These arms separate the atoms further and are afterwards redirected to merge the atoms again. This realizes a structure similar to a Mach-Zehnder interferometer.

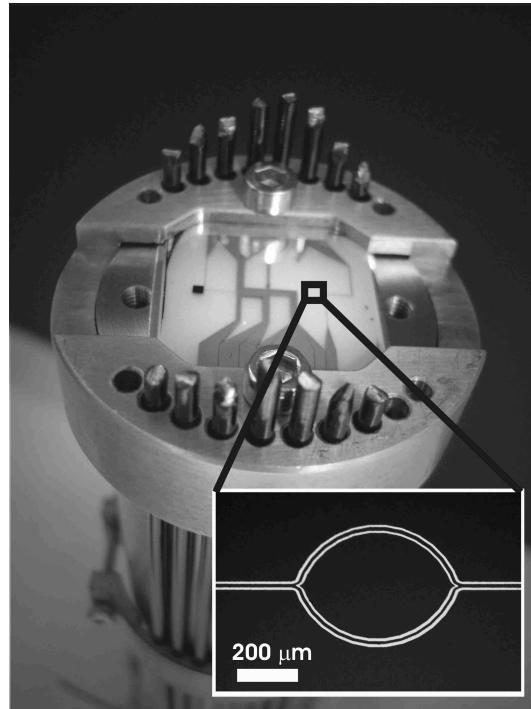


**Figure 1.** Photograph of the microstructured superconducting atom chip (size  $20 \times 20 \text{mm}^2$ ) designed for atom trapping and manipulating, recorded before contacting the chip wires. The magnified picture shows the interferometer structure recorded with an optical microscope.

A major challenge of current carrying chip based atom interferometers is the observed fragmentation of Bose-Einstein Condensates (BECs) close to the wires [23, 24]. Experimental investigations show that this is caused by corrugations of the current carrying wires [25]. This limitation has recently been suppressed to some extent by optimization of the chip fabrication process [26] or with the use of alternating currents [27]. With our epitaxially grown structure operated in the superconducting state we expect a significant reduction of the fragmentation effect.

These intriguing new experimental possibilities are the focus of the work with our HTS atom chip shown in figure 1. In section 2 we present the important material properties of the employed superconductor. We compare different fabrication techniques for the atom chip with regard to the quality and achievable size of structures. Finally we discuss the expected fragmentation of ultra-cold atoms for our atom chip based on the measured wire corrugations and roughness. In section 3 we discuss the design of the Mach-Zehnder type geometry by using two-wire guides including a closed persistent current loop. We present numerical simulations of the guiding potential based on a finite elements method which are used for optimization of the potential. Finally, we give an outlook for first experiments with the presented atom chip and conclude in section 4.

## 2. Properties of the atom chip

### 2.1. Superconducting material properties

The basis of the atom chip is a thin film of  $\text{YBa}_2\text{Cu}_3\text{O}_{7-x}$  (YBCO) on a Yttria-Stabilized Zirconia (YSZ) single crystalline substrate. The thin films used in our experiment typically have a critical temperature  $T_c$  of about 87K, depending on the exact composition of the YBCO. This working temperature can be generated by using liquid nitrogen as the coolant. This is a significant technical advantage compared to non-HTS materials where the critical temperature can only be achieved with liquid helium. This means the requirements for the cryogenic setup become much less stringent by using HTSs which is an important factor in the complex experimental setup of a typical ultra cold atom experiment. In our case the critical current density  $J_c$  at liquid nitrogen temperature is  $2 \text{ MA/cm}^2$ . For typical structure sizes on an atom chip with cross sections of  $100 \mu\text{m}^2$  this results in an upper limit for the current of 2 A. This is a typical current value used for trapping in various trap types on atom chips [3].

Connected with the critical current density are the two critical magnetic fields  $B_{c1,c2}$  of the type-II superconductor. Just like  $T_c$ , these parameters also crucially depend on the exact composition of the YBCO. While  $B_{c1}$  is typically on the order of tens of mT,  $B_{c2}$  can be as high as hundreds of T [28]. Both these values support the application of YBCO in atom chip structures where the employment of external magnetic fields has to be taken into account. The externally generated fields are usually on the order of a few mT, thereby reducing the critical current density only by a minor amount. For example, the external offset field in our experiment required for the realization of a Ioffe Pritchard type trap with a Z-shaped wire [29] will be 6 mT. However, for future studies, such as suggested in [30], we can tune the superconducting state from the Meissner to the Shubnikov phase by applying the required offset magnetic field.

YBCO has been one of the most widely studied HTSs. To date, there are HTSs which possess even better properties than YBCO concerning one or more of the relevant parameters discussed above. However, the choice of the HTS is determined by the well developed micro-structure fabrication techniques and structural properties of this thin film.

### 2.2. Fabrication of the atom chip

The manufacturing of the superconducting chip consists of two main steps which are the fabrication of the HTS chip and its structuring. The YBCO is grown by epitaxy as a thin film on a YSZ substrate. The lattice constants of YBCO and YSZ are matched, allowing homogeneous growth of the superconducting material. Another important factor is the matching of the temperature expansion coefficient of the film and substrate. The atom chip is subjected to stress by temperature changes of approximately 200-300K in a short period of time (<5 min). A mismatch would result in cracks of the superconducting film. The final thickness of the YBCO film is 600-800nm, possessing a surface with a

negligible roughness determined by the epitaxial growth as discussed in section 2.3. On top of the YBCO film a 200nm thick layer of gold is deposited. This film decreases the electrical contact resistance. This is important when the ceramic based superconductor is contacted to metallic electrodes supplying the currents for the generation of the magnetic fields. Furthermore, the gold film protects the superconducting material.

Structuring of the chip is performed by two different techniques. These are standard optical lithography followed by a wet-chemical etching as well as direct femtosecond (fs) laser ablation. The standard lithography procedure has a resolution limit of about  $1\mu\text{m}$  for the structure size. With the fs-laser ablation procedure the desired patterns on the chip are realized by locally removing the Gold and YBCO layer with focused laser pulses ( $2\mu\text{J}$ , 130 fs, center wavelength 800nm), resulting in insulating regions between the superconducting structures. In this laser assisted structuring technique it is crucial that the film is not heated. Due to heating oxygen would be lost and the superconducting properties of the thin film would degrade. This requirement sets the demand for using fs-laser pulses.

We compared the two methods of lithography and fs-laser machining by measuring the roughness of the realized structures as will be discussed in section 2.3. We find that the structures machined with standard lithographic techniques have a lower roughness than the structures machined with the fs-laser. However, the laser ablation is used in subsequently optimizing of imperfect regions of our lithographically machined chips.

Additionally, we plan to employ e-beam lithography and ion-milling [31] allowing for structure sizes less than  $1\mu\text{m}$ . These small sizes will allow the fabrication of more complex structures and the optimization of critical areas in the interferometer structure.

### 2.3. Roughness of the guiding structure

The fragmentation of BECs and thermal atomic clouds trapped at distances  $\leq 100\mu\text{m}$  from the current carrying wires has been independently observed in several experiments on normal conducting atom chips [23, 24]. Since the atoms will be held at a typical distance of  $5\mu\text{m}$  from the wires forming the guide presented in this paper, these effects have to be taken into account. The fragmentation is mainly caused by geometric distortions of the current flow from the anticipated path in the conductor, inducing an overall potential roughness [25]. Corrugations of the wire edges have been identified as the main contribution to these distortions [32]. Besides the employment of time-varying fields [27], substantial effort has been undertaken for optimizing the fabrication process allowing for a suppression of the potential roughness. In this respect, our atom chip meets the relevant criteria for a successful implementation of optimal fabrication processes. The chip structures are written by optical lithography [33] which has been shown to reduce the roughness by two orders of magnitude [34, 35]. To characterize the roughness of our chip we performed measurements of the edges and surfaces of the superconducting wires with an atomic force microscope, shown in figure 2. The edges of the wires feature structures with typical sizes of about 200nm, which is comparable to

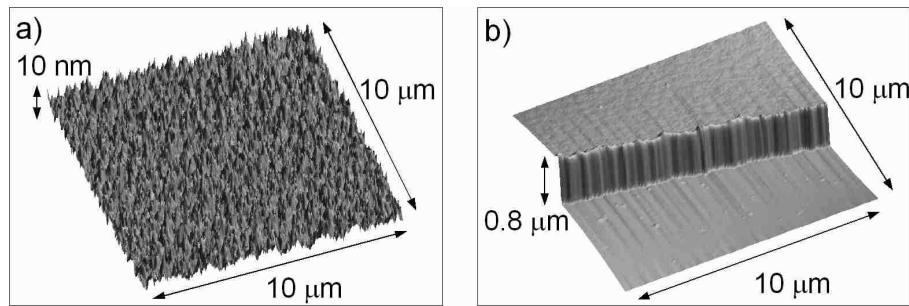


**Figure 2.** Images of different areas with sizes of  $100\mu m^2$  of the superconducting chip taken by atomic force microscopy (AFM). a) Scan above a flat surface of a superconducting wire. b) Scan of a wire edge. Note the different scales of the height amplitude. The straight lines visible in part b) appear artificially in the AFM measurement in the moving direction of the scanning tip induced by the comparatively large height difference at the edge.

the grain size limit of 100nm measured in [35]. Moreover, we measured the roughness of the surface of the wire, which can also contribute to the overall potential distortion. We find the roughness of the surface almost negligible with a rms value of the surface height of only 2.3 nm. We explain this small roughness by one important intrinsic advantage of YBCO, which is the epitaxial growth of the superconducting film. The epitaxial growth of YBCO prevents basically all graining effects during the fabrication. This graining has been identified to limit the achievable conductor quality [35]. We attribute the residual surface roughness to the gold film, possibly allowing to achieve values below 1 nm for bare YBCO surfaces.

Beyond the known fabrication optimization procedure, our atom chip promises further suppression of the fragmentation effect. As pointed out in [34, 35], for wires fabricated with optimized procedures, inhomogeneities in the bulk material contribute to the potential roughness as well. A recent study demonstrated that scattering at inhomogeneities with different conductivity can become the dominating effect [36]. Therefore we anticipate a substantial reduction of this contribution due to the resistance free current flow in the superconductor.

### 3. Two-wire guide Mach-Zehnder interferometer structure

Figure 1 shows the pattern realized for the chip structure. The heart of the chip is a lemon shaped closed loop. This structure is designed so that a persistent current can flow inside the loop. With this loop a novel two wire guide geometry in a Mach-Zehnder-type interferometer structure has been realized, schematically shown in Figure 3. This unique design ensures a symmetric splitting and symmetric recombination process which is desirable for an interferometer type structure.

The guiding potential of this configuration is generated by two parallel conductors carrying opposite currents and magnetic offset fields perpendicular to the chip surface

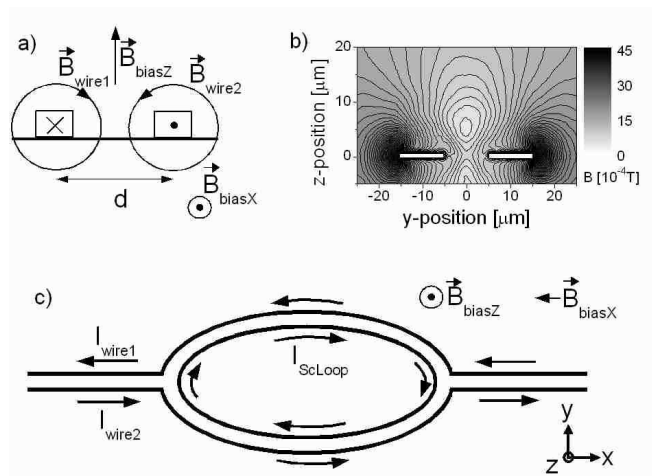


**Figure 3.** Schematic of the two-wire guiding potential realizing a Mach-Zehnder interferometer-type geometry. The principle of the two-wire guide using opposing currents and bias magnetic fields  $B_{biasX}$  and  $B_{biasZ}$  is sketched in a). In b) the simulated magnetic field along the guide with wire currents of 55mA and  $B_{biasZ} = 1.53$  mT,  $B_{biasX} = 0.3$  mT is shown. This basic guiding potential is transformed to an interferometer type guiding structure by enclosing a third wire in the form of a closed superconducting loop as shown in c). This type of guiding potential is obtained with opposing currents  $I_{wire1}$  and  $I_{wire2}$  and a persistent super current  $I_{ScLoop}$  of the same magnitude, which is always directed opposite to the current in the neighboring wire.

and along the wires, similar to [11]. This results in a magnetic field minimum above the chip surface (figure 3). In this field minimum atoms can be guided. Our guide is realized by two wires with widths of  $10\mu m$  which are separated by a distance of  $d=10\mu m$ . Typical values for our geometry are currents of 55mA in each wire and bias magnetic fields of  $B_{biasZ} = 1.53$  mT and  $B_{biasX} = 0.3$  mT. This leads to oscillation frequencies for  $^{87}Rb$  in the  $|F = 2, m_F = 2\rangle$  state of  $\nu_y=9.1$  kHz in  $y$ - and  $\nu_z=8.2$  kHz in  $z$ -direction. This two wire guide can be extended to a beam-splitter in the shape of a Y-junction by using a third wire carrying a current always opposing the current of the neighboring wire as suggested in [37]. The Y-junction formed with this two wire guide prevents undesired loss channels. Additionally it minimizes changes in the guiding potential present in Y-junctions made of single-wire guides. Unfortunately, with normal conducting wires in a planar geometry the simple extension of this configuration into an interferometer type topology made out of two opposing Y-junctions is not possible, since the wires have to be connected to an external current source. This drawback is overcome in our novel guiding design, where the third wire placed between the two Y-junctions is formed in a closed loop. By inducing a persistent current in this loop we can realize a Mach-Zehnder-type interferometer structure.

To investigate the properties of the interferometer structure we perform a numerical analysis by a finite elements method. The local current density in the wires is calculated which leads to the magnetic field distribution. In combination with the additional

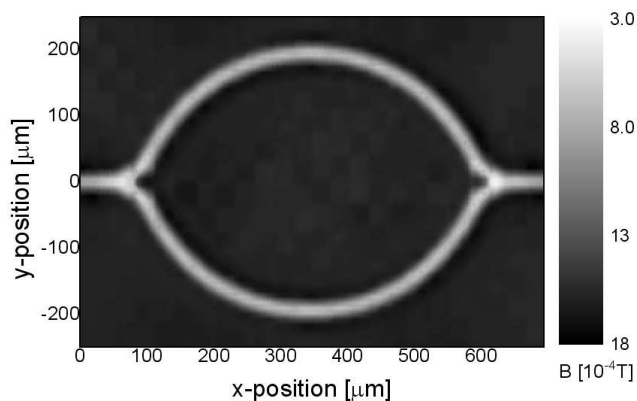


**Figure 4.** Calculated absolute magnetic field in the x-y-plane at the height of the potential minimum in the bare two-wire guide.

bias magnetic fields this results in the guiding confinement for the atoms. In this calculation we approximate the superconductor with effectively zero resistance and magnetic insulation. To verify these approximations we compare it to simulations based on the London equations and find no significant deviation in the guiding potential.

The structure of the guiding wires is optimized in order to minimize changes in the guiding potential, in particular the transverse oscillation frequencies near the separation point. These are the main optimization criteria since a vanishing confinement at the separation point had been identified to cause excitation into higher modes in a formerly demonstrated beam-splitter on an atom chip leading to a random phase in matter-wave interference [20]. For the optimization, we vary the values of the currents in the wires as well as the offset magnetic bias fields for finding optimal guiding properties. Additionally, the shape of the superconductor is optimized in order to decrease the current density at sharp edges. The ratio of the current density between the areas at the tip of the loop and the linear part is approximately two in the optimized geometry. Note that if the local current density is reaching the critical value the superconducting properties can be lost. After the separation point, our structure has the shape of two separated two-wire guides in the form of half-ellipses.

The obtained numerical simulations of the guiding structure for  $^{87}\text{Rb}$  atoms are shown in Figs. 4 and 5. Figure 4 shows the absolute value of the magnetic field in the x-y-plane above the surface of the wires at a height  $z=5.3\mu\text{m}$ . This corresponds to the height of the potential minimum of the bare two-wire guide. In figure 5 we show the potential in y-direction for three chosen lines along the guide in x-direction at a height  $z=5.2\mu\text{m}$ . The calculated trapping frequencies in y-direction for different x-positions near the separation point are shown in figure 6. Additionally we show in figure 6 the distance between the two potential minima depending on the x-position after

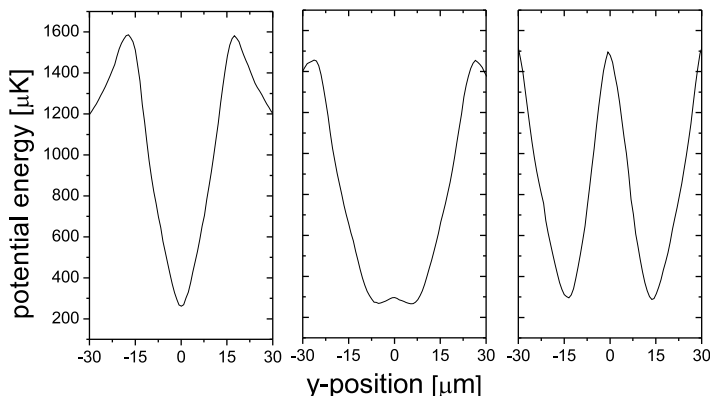


**Figure 5.** Potential energy for  $^{87}\text{Rb}$  along the  $y$ -axis in splitting direction for three different  $x$ -positions displayed as a temperature  $T = E/k_B$  for a height  $z=5.2\mu\text{m}$  where  $k_B$  is the Boltzmann constant. The  $x$ -positions correspond to a single guide, two guides shortly after the separation point and two isolated atom guides, respectively. (From left to right:  $x=47.3\mu\text{m}$ ,  $69.1\mu\text{m}$ ,  $81\mu\text{m}$ .)

the separation. At the separation point the field minimum is at a height  $z=3.8\mu\text{m}$  and the oscillation frequencies are  $\nu_y=0.9$  kHz in  $y$ - and  $\nu_z=3.4$  kHz in  $z$ -direction. Hence, we find strong confinement and non-vanishing magnetic field at the separation point. For longitudinal atomic velocities on the order of mm/s the adiabaticity of the splitting described by the quantity  $(1/\nu_y^2)(\partial\nu_y/\partial x)(\partial x/\partial t)$  [20] can be ensured. Therefore we estimate the potential change not to be a limiting factor for the splitting process. After full separation the potential of the guides in the two arms equals the potential of the single two-wire guide. Due to the applied offset magnetic field we obtain a vanishing magnetic field at the merging point of the two arms. However, the influence of the magnetic field zero is not essential for the interferometer, since the atoms can be released from the guiding potential before reaching the absolute field minimum. After the separation point the minimum of the guiding potential is decreasing in propagation direction by 0.2mT with a maximum gradient which is one order of magnitude smaller than the gradient in confinement direction. Therefore, we do not expect excitation to higher transverse modes in the curved guiding structure.

To ensure the symmetry of the guiding potential, the current for the two outer wires will be applied in series, which also minimizes the relative current noise. To adjust the current in the closed loop we plan to employ spectroscopy of atoms brought close to the wires. A slight mismatch between the currents in the outer wires and the inner wire will not change the inherent symmetry of the interferometer structure.

The initialization of the atom guide and especially the persistent current will be performed in a controlled temporal sequence by changing the chip temperature and tuning the applied magnetic fields. The persistent current in the closed loop can be controlled to high precision by changing the offset magnetic field as presented in [15].

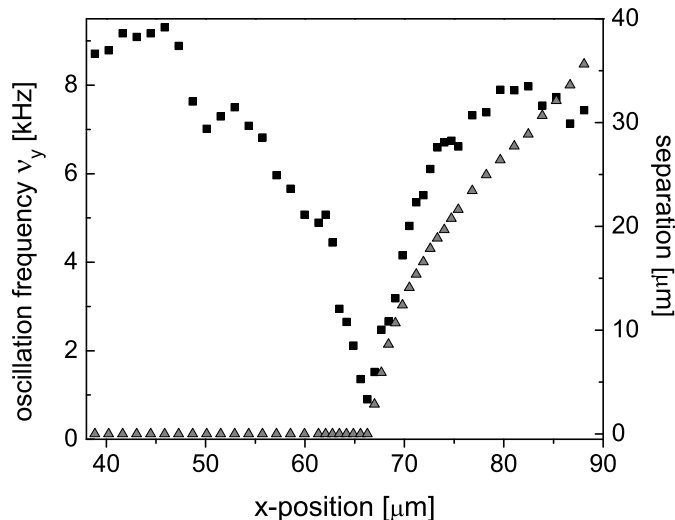


**Figure 6.** Y-direction trapping frequency along the x-direction near the separation point at the first Y-junction (boxes) and separation distance between the two potential minima of the guide (triangles). For x-positions before the separation point at  $x=66.3\mu\text{m}$  the calculation shows the trapping frequency of a single atom guide, while after the separation point the trapping frequencies in each of the two identical guiding arms are shown.

Additionally, in our setup we can tune the persistent current with the two half-loop wires of the interferometer guide itself. Initially, the atoms will be prepared in a Z-shaped Ioffe-Pritchard type magnetic trap which is embedded in our superconducting atom chip (figure. 1). Subsequently, the atoms will be loaded into the wave guide by switching between different wire connections.

The stable operation of the interferometer type structure demands well-defined control of the magnetic offset fields since field changes will induce current changes in the superconducting loop. To reach a current stability of better than 0.01 in the closed loop (inductance  $L \approx 0.3\text{nH}$ ) the magnetic bias field  $B_{BiasZ}$  has to have a stability of better than  $1\mu\text{T}$ . Therefore, this requirement demands a relative magnetic field stability of approximately  $10^{-3}$  which can routinely be achieved in ultra-cold atoms experiments.

In first experiments with the guiding structure we will investigate the splitting process of ultra-cold atoms at the Y-junctions, in particular its efficiency including undesired reflection and most importantly its coherence properties. The observations of ultra-cold atoms can be performed using standard time-of-flight absorption imaging, allowing the overlapping of split atomic clouds. For this the atoms can be released from the wave guide by switching off the current in the wires and the superconducting loop. The persistent current in the closed loop can be changed by switching on an appropriate magnetic offset field. The final operation of the interferometer type structure consists of splitting, spatially diverging and finally recombining of ultra-cold atoms.

Our setup allows the evaluation of employing thermal atoms as well as quantum degenerate gases in the interferometer structure. By using a BEC the macroscopic matter wave characteristic is favorable, but may be limited by phase fluctuations in elongated condensates as measured in [38, 39]. Alternatively, single particle interference can be employed with thermal atoms, where one can in principle investigate multi mode operation, similar to [40].

One major motivation in the field of guided atom interferometry is their potential as compact and precise inertial sensors [3]. In this respect, especially the development of precision matter wave gyroscopes operated with guided atoms is in the focus of current research due to the promising realization of large enclosed areas for enhancing their sensitivity [41]. Our current guiding potential encloses an area of about  $0.17 \text{ mm}^2$ . An atom interferometer operated with  $^{87}\text{Rb}$  enclosing this area already experiences a phase shift for rotations of  $33\text{mrad}/\Omega_{\text{earth}}$  due to the Sagnac effect, where  $\Omega_{\text{earth}} = 7.3 \cdot 10^{-5}\text{rad/s}$  is the rotation velocity of the earth. However, the enclosed area can in principle easily be scaled up, enhancing the sensitivity even further.

In future experiments it might be interesting to operate the guide at higher wire currents and with higher bias magnetic fields. Consequently, tighter confinement can be achieved by employing thin wires while maintaining a high current. In this respect, superconductors offer an advantage compared to normal conductors since they can provide current densities of more than  $10^7\text{A/cm}^2$  without heat dissipation. To evaluate the limits of confinement of our atom chip, we measured the critical current density at different temperatures of the chip shown in figure 7. We find a nearly linear increase in the critical current density for decreasing temperatures up to the current limit of our measurement device. Our current setup allows the possibility to use liquid helium as a coolant as well. To estimate the critical current density at 4.2K, we conservatively follow the behavior given by  $J_c(T) = J_c(0) \cdot [1 - (T/T_c)^2]$ . We find a critical current density of  $13(1)\text{MA/cm}^2$ .

This current density allows to operate a  $1\mu\text{m}$  wide wire with a current of 60mA whereas the further reduction of the critical current density by accordingly increased bias magnetic fields has been taken into account.  $^{87}\text{Rb}$  atoms trapped with these parameters in a single wire guide at a distance of  $1\mu\text{m}$  would experience a trapping frequency of  $\nu=465 \text{ kHz}$ . This trapping frequency corresponds to a Lamb-Dicke-parameter  $\eta = \sqrt{\frac{\omega_{\text{rec}}}{\nu}}$  of 0.23 when interacting with laser light with a wave vector  $k=2\pi/\lambda = 2\pi/780\text{nm}$ , where  $\omega_{\text{rec}} = \hbar k^2/2m$  is the recoil frequency. This is an interesting regime for further applications such as for example quantum information operations [42].

#### 4. Conclusions

In this paper we have presented a novel interferometer type guiding structure based on a closed superconducting loop. The presented guiding potential has been optimized with respect to critical parameters near the splitting regions of matter waves. The interferometer type guide has the potential to overcome limitations which current room

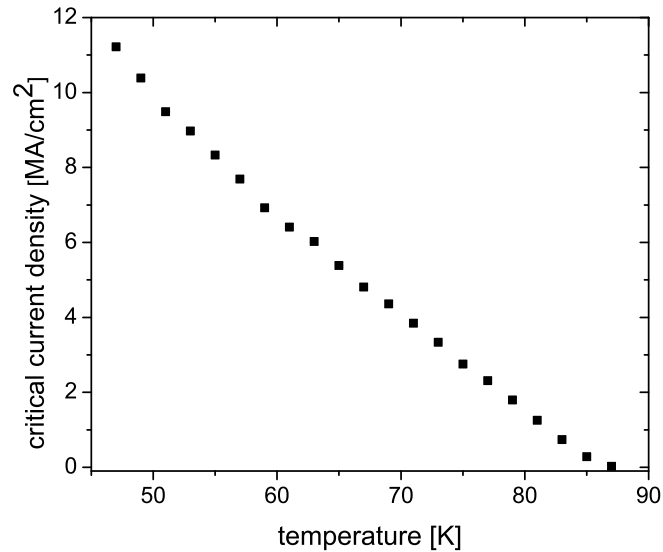


**Figure 7.** Measurement of the temperature dependent critical current density of a  $26 \mu\text{m}$  wide wire. For lower temperatures the measurement is limited by the maximum obtainable current of 2A of the employed measurement system. The transition to superconductivity occurs at 87.1K.

temperature atom chip devices are facing. One example is the fragmentation of atomic clouds close to the chip surface. Currently, numerical simulations of the propagation of atomic matter waves in the presented guiding structures are being performed for a further optimization of the second generation superconducting chip devices. At present, the superconducting atom chip is integrated into our cryogenic experimental setup for the generation of quantum-degenerate gases. The enormous potential offered by the combination of superconducting solid state systems with neutral atoms will allow a variety of novel experiments, which will not only be limited to high temperature superconductors. These are for example the probing of vortices in superconducting films with neutral atoms [30], the coupling of the magnetic moment of ultra-cold atoms to superconducting quantum interference devices [43] and the quantum state transfer between solid state and atomic quantum systems [1, 2]. However, this type of experiments faces severe technical challenges which will partially be evaluated with the presented system.

## Acknowledgments

We thank C. H. Oh for his kind support. Additionally, we thank L. Wang for assistance regarding the critical current density measurements. This work is funded by the Nanyang Technological University (grant no. WBS M58110036) and by A-Star (grant no. SERC 072 101 0035 and WBS R-144-000-189-305).

## References

- [1] Sørensen A S, van der Wal C H, Childress L I and Lukin M D 2004 *Phys. Rev. Lett.* **92** 063601
- [2] André A, DeMille D, Doyle J M, Lukin M D, Maxwell S E, Rabl P, Schoelkopf R J and Zoller P 2006 *Nature Phys.* **2** 636
- [3] Fortágh J and Zimmermann C 2007 *Rev. Mod. Phys.* **79** 235
- [4] Folman R, Krüger P, Schmiedmayer J, Denschlag J and Henkel C 2002 *Adv. At. Mol. Opt. Phys.* **48** 263
- [5] Fortagh J, Grossmann A, Zimmermann C and Hänsch T W 1998 *Phys. Rev. Lett.* **81** 5310
- [6] Vuletic V, Fischer T, Praeger M, Hänsch T W and Zimmermann C 1998 *Phys. Rev. Lett.* **80** 1634
- [7] Birkl G, Buchkremer F B J, Dumke R and Ertmer W 2001 *Opt. Comm.* **191** 67
- [8] Hänsel W, Hommelhoff P, Hänsch T W and Reichel J 2001 *Nature* **413** 498
- [9] Aubin S, Myrskog S, Extavour M H T, LeBlanc L J, McKay D, Stummer A and Thywissen J H 2006 *Nature Phys.* **2** 384
- [10] Denschlag J, Cassetari D and Schmiedmayer J 1999 *Phys. Rev. Lett.* **82** 2014
- [11] Dekker N H, Lee C S, Lorent V, Thywissen J H, Smith S P, Drndić M, Westervelt R M and Prentiss M 2000 *Phys. Rev. Lett.* **84** 1124
- [12] Hänsel W, Reichel J, Hommelhoff P and Hänsch T W 2001 *Phys. Rev. Lett.* **86** 608
- [13] Calarco T, Hinds E A, Jaksch D, Schmiedmayer J, Cirac J I and Zoller P 2000 *Phys. Rev. A* **61** 022304
- [14] Nirrengarten T, Qarry A, Roux C, Emmert A, Nogues G, Brune M, Raimond J-M and Haroche S 2006 *Phys. Rev. Lett.* **97** 200405
- [15] Mukai T, Hufnagel C, Kasper A, Meno T, Tsukada A, Semba K and Shimizu F 2007 *Phys. Rev. Lett.* **98** 260407
- [16] Roux C, Emmert A, Lupascu A, Nirrengarten T, Nogues G, Brune M, Raimond J-M and Haroche S 2008 *Europhys. Lett.* **81** 56004
- [17] Berman P 1997 *Atom Interferometry* (San Diego: Academic Press)
- [18] Wang Y-J, Anderson D Z, Bright V M, Cornell E A, Diot Q, Kishimoto T, Prentiss M, Saravanan R A, Segal S R and Wu S 2005 *Phys. Rev. Lett.* **94** 090405
- [19] Schumm T, Hofferberth S, Andersson L M, Wildermuth S, Groth S, Bar-Joseph I, Schmiedmayer J and Krüger P 2005 *Nature Phys.* **1** 57
- [20] Shin Y, Sanner C, Jo G-B, Pasquini T A, Saba M, Ketterle W, Pritchard D E, Vengalattore M and Prentiss M 2005 *Phys. Rev. A* **72** 021604(R)
- [21] Hofferberth S, Lesanovsky I, Fischer B, Verdu J and Schmiedmayer J 2006 *Nature Phys.* **2** 710
- [22] Kreutzmann H, Poulsen U V, Lewenstein M, Dumke R, Ertmer W, Birkl G and Sanpera A 2004 *Phys. Rev. Lett.* **92** 163201
- [23] Fortágh J, Ott H, Kraft S, Günther A and Zimmermann C 2002 *Phys. Rev. A* **66** 041604
- [24] Leanhardt A E, Shin Y, Chikkatur A P, Kielpinski D, Ketterle W and Pritchard D E 2003 *Phys. Rev. Lett.* **90** 100404
- [25] Wang D-W, Lukin M D and Demler E 2004 *Phys. Rev. Lett.* **92** 076802
- [26] Schumm T, Estève J, Figl C, Trebbia J-B, Aussibal C, Nguyen H, Mailly D, Bouchoule I, Westbrook C I and Aspect A 2005 *Euro. Phys. J. D* **32** 171
- [27] Trebbia J-B, Garrido Alzar C L, Cornelussen R, Westbrook C I and Bouchoule I 2007 *Phys. Rev. Lett.* **98** 263201
- [28] NIST online database Electronic address: [www.nist.gov/srd](http://www.nist.gov/srd)
- [29] Denschlag J, Cassetari D, Chenet A, Schneider S and Schmiedmayer J 1999 *Appl. Phys. B* **69** 291
- [30] Scheel S, Fermani R and Hinds E A 2007 *Phys. Rev. A* **75** 064901
- [31] Della Pietra L, Aigner S, vom Hagen C, Groth S, Bar-Joseph I, Lezec H J and Schmiedmayer J 2007 *Phys. Rev. A* **75** 063604
- [32] Estève J, Aussibal C, Schumm T, Figl C, Mailly D, Bouchoule I, Westbrook C I and Aspect A 2004 *Phys. Rev. A* **70** 043629

- [33] Groth S, Krüger P, Wildermuth S, Folman R, Fernholz T, Schmiedmayer J, Mahalu D and Bar-Joseph I 2004 *Appl. Phys. Lett.* **85** 2980
- [34] Krüger P, Wildermuth S, Hofferberth S, Andersson L M, Groth S, Bar-Joseph I and Schmiedmayer J 2005 *J. Phys. Conf. Series* **19** 56
- [35] Krüger P, Andersson L M, Wildermuth S, Hofferberth S, Haller E, Aigner S, Groth S, Bar-Joseph I and Schmiedmayer J 2007 *Phys. Rev. A* **76** 063621
- [36] Aigner S, Della Pietra L, Japha Y, Entin-Wohlman O, David T, Salem R, Folman R and Schmiedmayer J 2008 *Science* **319** 1226
- [37] Cassettari D, Chenet A, Folman R, Haase A, Hessmo B, Krüger P, Maier T, Schneider S, Calarco T and Schmiedmayer J 2000 *Appl. Phys. B* **70** 721
- [38] Hofferberth S, Lesanovsky I, Fischer B, Schumm T and Schmiedmayer J 2007 *Nature* **449** 324
- [39] Jo G-B, Choi J-H, Christensen C H, Lee Y-R, Pasquini T-A, Ketterle W and Pritchard D E 2007 *Phys. Rev. Lett.* **99** 240406
- [40] Andersson E, Calarco T, Folman R, Andersson M, Hessmo B and Schmiedmayer J 2002 *Phys. Rev. Lett.* **88** 100401
- [41] Wu S, Su E and Prentiss M 2007 *Phys. Rev. Lett.* **99** 173201
- [42] Jaksch D, Briegel H-J, Cirac J I, Gardiner C W and Zoller P 1999 *Phys. Rev. Lett.* **82** 1975
- [43] Walraven J T M and Silvera I F 1981 *Physica* **107B** 515